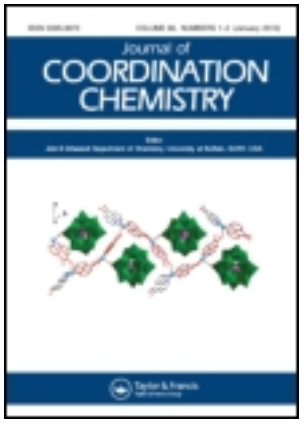

Journal of Coordination Chemistry
Publication details, including instructions for authors and subscription information:
http://www.tandfonline.com/loi/gcoo20

Synthesis, crystal structure, fluorescence, electrochemical property, and SOD-like activity of an unexpected nickel(II) complex with a quinazoline-type ligand

Lan-Qin Chai[a], Gang Liu[a], Yu-Li Zhang[a], Jiao-Jiao Huang[a] & Jun-Feng Tong[b]

[a] School of Chemical and Biological Engineering, Lanzhou Jiaotong University, Lanzhou, P.R. China

[b] Key Laboratory of Opto-Electronic Technology and Intelligent Control, Lanzhou Jiaotong University, Ministry of Education, Lanzhou, P.R. China

Accepted author version posted online: 21 Oct 2013.Published online: 26 Nov 2013.

To cite this article: Lan-Qin Chai, Gang Liu, Yu-Li Zhang, Jiao-Jiao Huang & Jun-Feng Tong (2013) Synthesis, crystal structure, fluorescence, electrochemical property, and SOD-like activity of an unexpected nickel(II) complex with a quinazoline-type ligand, Journal of Coordination Chemistry, 66:22, 3926-3938, DOI: 10.1080/00958972.2013.857016

To link to this article: http://dx.doi.org/10.1080/00958972.2013.857016

Journal of Coordination Chemistry, 2013
Vol. 66, No. 22, 3926–3938, http://dx.doi.org/10.1080/00958972.2013.857016

Synthesis, crystal structure, fluorescence, electrochemical property, and SOD-like activity of an unexpected nickel(II) complex with a quinazoline-type ligand

LAN-QIN CHAI*†, GANG LIU†, YU-LI ZHANG†, JIAO-JIAO HUANG† and JUN-FENG TONG‡

†School of Chemical and Biological Engineering, Lanzhou Jiaotong University, Lanzhou, P.R. China
‡Key Laboratory of Opto-Electronic Technology and Intelligent Control, Lanzhou Jiaotong University, Ministry of Education, Lanzhou, P.R. China

(*Received 17 May 2013; accepted 8 October 2013*)

An unexpected mononuclear Ni(II) complex, $[Ni(L^2)_2]\cdot CH_3OH$ (HL^2 = 1-(2-{[(*E*)-3,5-dichloro-2-hydroxybenzylidene]amino}phenyl)ethanone oxime), has been synthesized via complexation of Ni(II) acetate tetrahydrate with HL^1. HL^1 and its corresponding Ni(II) complex were characterized by IR, ^{1}H-NMR spectra, HRMS, as well as by elemental analysis, UV–vis, and emission spectroscopy. The crystal structure of the complex has been determined by single-crystal X-ray diffraction. Each complex links two other molecules into an infinite 1-D chain via intermolecular hydrogen bonds. Moreover, the electrochemical properties of the nickel complex were studied by cyclic voltammetry. Superoxide dismutase-like activities of HL^1 and Ni(II) complex were also investigated.

Keywords: Quinazoline-type ligand; Crystal structure; Fluorescence behavior; Cyclic voltammetry; Superoxide dismutase activity

1. Introduction

Oxime-type compounds are versatile ligands in coordination chemistry. A number of complexes with oxime-type ligands have been reported with interesting structures and potential applications [1]. For example, Dilber *et al.* [2] report a new macrobicyclic vic-dioxime and macrobicyclic groups might have selective ion binding properties and could be used for remediation of heavy metal pollution or recovery of precious metals from heavy metal wastes. The quinazoline ring system along with many alkaloids is widely recognized in inorganic syntheses and medicinal applications [3], for example, in HIV reverse transcriptase inhibitors [4]. Some of them or their metal complexes are used as biological models in understanding the structure of biomolecules and biological processes [5–7]. Such compounds have become the center of creating new drugs, some with highly active compounds have been commercialized such as fungicide fuquinconazole, anti-cancer drug, antihypertensive pyrazosin, etc. [8–10]. Some transition metal complexes with quinazoline analogs have been investigated in coordination chemistry and biological

*Corresponding author. Email: dongwk@mail.lzjtu.cn

chemistry, although much remains to be understood [11, 12]. Nickel(II) complexes with oxime-type ligands have been widely investigated in coordination chemistry and biological chemistry [2, 13–15], but cleavage of two C–N bonds of Schiff bases have not been observed in reaction with metal salts.

In this paper, we report the synthesis, structural characterization, and fluorescence of a mononuclear Ni(II) complex, $[Ni(L^2)_2]\cdot CH_3OH$, which is an unexpected mononuclear Ni (II) complex possessing a Schiff base-type Ni–N_4O_2 instead of an anticipated quinazoline-type Ni–N_4O_2 complex. Fluorescence of the Ni(II) complex in DMF solution is also investigated; electrochemistry and superoxide dismutase (SOD) activity are also described.

2. Experimental

2.1. *Materials and physical measurements*

All chemicals were of analytical reagent grade from Tianjin Chemical Reagent Factory and used without purification. C, H, and N analyzes were obtained using a GmbH VarioEL V3.00 automatic elemental analysis instrument. Elemental analysis for Ni was determined by an IRIS ER/S·WP-1 ICP atomic emission spectrometer. IR spectra were recorded on a Vertex70 and Nicolet Instrument Corporation NEXUS 670 FT-IR spectrophotometer, with samples prepared as KBr (500–4000 cm^{-1}) and CsI (100–500 cm^{-1}) pellets. UV–vis absorption spectra were recorded on a Shimadzu UV-2550 spectrometer. The fluorescence spectrum was taken on a 970 CRT spectrofluorometer (Spectro, Shanghai). Cyclic voltammetry measurements were performed using a Chi660 (The United States CHI) voltammetric analyzer, a three electrode arrangement made up of a glassy carbon working electrode, a platinum wire auxiliary electrode, and a Ag/AgCl reference electrode was used in DMF containing 0.05 $M\,L^{-1}$ tetrabutylammonium perchlorate at scan rates of 100 $mV\ s^{-1}$. ^1H NMR spectra were determined on a Mercury plus (400 or 300 MHz) instrument using $CDCl_3$ as solvent and TMS as internal standard. MS (ESI) were measured on a Bruker Esquire 6000 mass spectrometer. Single-crystal X-ray structure determination was carried out on a Bruker Smart 1000 CCD area detector diffractometer. Melting points were obtained by use of a microscopic melting point apparatus made by Beijing Taike Instrument Limited Company and are uncorrected.

2.2. *Preparation of HL^1 and its complex*

2.2.1. Synthesis and structural characterization of HL^1. The synthetic route of quinazoline-type ligand (HL^1) is shown in scheme 1.

(*E*)-1-(2-Aminophenyl)ethanone oxime was synthesized as white powder according to an analogous method reported earlier [16, 17]. Yield 94.7%; m.p. 106–107 °C. Anal. Calcd for $C_8H_{10}N_2O$ (Mw 150.18) (%): C, 63.98; H, 6.71; N, 18.65. Found (%): C, 64.24; H, 6.58; N, 18.83. IR (KBr) $\nu\,cm^{-1}$: 3389 (N–OH), 3248 (N–H), 3133 (Ar–H), 1602 (C=N). ^1H NMR (300 MHz, $CDCl_3$): 11.30 (s, 1H, NOH), 7.63–7.25 (m, 4H, ArH), 5.82 (s, 2H, NH_2), 2.56 (s, 3H, CH_3).

2-(3,5-Dichloro-2-hydroxyphenyl)-4-methyl-1,2-dihydroquinazoline 3-oxide: To an ethanol solution (4 mL) of 3,5-dichloro-2-hydroxybenzaldehyde (0.1909 g, 1.0 mM) was added an ethanol solution (4 mL) of (*E*)-1-(2-aminophenyl) ethanone oxime (0.1502 g,

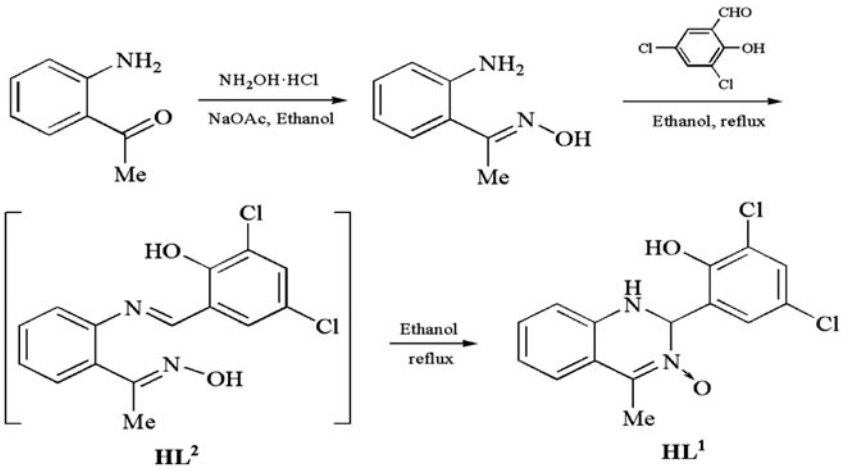

Scheme 1. Synthetic route of HL^1.

1.0 mM). After stirring at 55–60 °C for 12 h, the mixture was filtered, precipitates were collected on a suction filter to afford HL^1 (0.2315 g, 71.3%) as pale yellow powder [16]. m.p. 217–218 °C. ^{1}H NMR (400 MHz, $CDCl_3$) δ 13.59 (br, 1H, OH), 7.39 (dd, J = 7.6 Hz, J = 4.0 Hz, 1H, CH_{arom}), 7.33 (d, J = 7.6 Hz, 1H, CH_{arom}), 7.31 (d, J = 2.4 Hz, 1H, CH_{arom}), 7.11 (d, J = 2.4 Hz, 1H, CH_{arom}), 7.00 (d, J = 4 Hz, 1H, CH_{arom}), 6.99 (dd, J = 8.0 Hz, J = 4.0 Hz, 1H, CH_{arom}), 6.40 (br, 1H, NH), 4.95 (br, 1H, CH), 2.48 (s, 3H, CH_3). Anal. Calcd for $C_{15}H_{12}Cl_2N_2O_2$ (Mw 323.17) (m/z = 323.2) (%): C, 55.75; H, 3.74; N, 8.67. Found (%): C, 55.93; H, 3.97; N, 8.86.

2.2.2. Preparation of the Ni(II) complex. A solution of Ni(II) acetate tetrahydrate (0.0013 g, 0.005 mM) in methanol (2 mL) was added dropwise to a solution of HL^1 (0.0065 g, 0.01 mM) in dichloromethane (4 mL). The color of the mixing solution turned brown immediately from light yellow. The solvent was partially evaporated for one week at room temperature and several brown needle-like single crystals suitable for X-ray crystallographic analysis were obtained. Anal. Calcd for $C_{31}H_{26}Cl_4N_4NiO_5$ $[Ni(L^2)_2]\cdot CH_3OH$ (Mw 735.07) (%): C, 50.65; H, 3.57; N, 7.62; Ni, 7.98. Found (%): C, 50.78; H, 3.63; N, 7.67; Ni, 7.93.

2.3. *X-ray structure determination of [Ni(L2)2]·CH3OH*

The X-ray diffraction measurement for the Ni(II) complex was performed on a Bruker Smart 1000 CCD diffractometer with graphite-monochromated Mo-Kα radiation (λ = 0.71073 Å) at 298(2) K. Data reduction and cell refinement were performed using SAINT [18]. The structure was solved by direct methods (SHELXS-97) and subsequent difference-Fourier map revealed positions of the remaining atoms, and all non-hydrogen atoms were refined anisotropically using full-matrix least-squares on F^2 with SHELXL-97 [19, 20]. Anisotropic thermal parameters were assigned to all non-hydrogen atoms. The hydrogens were generated geometrically. Crystallographic data and structural refinements for the Ni(II) complex are listed in table 1.

Table 1. Crystallographic data and data collection parameters for $[Ni(L^2)_2]\cdot CH_3OH$.

Empirical formula	$C_{31}H_{26}Cl_4N_4NiO_5$
Formula weight	735.07
Temperature (K)	298(2)
Wavelength (Å)	0.71073
Crystal system	Monoclinic
Space group	$P2_1/c$
Unit cell dimensions (Å, °)	
a	22.436(2)
b	7.7150(5)
c	19.0950(18)
β	109.798(2)
Volume (Å^3), Z	3109.9(5), 4
Calculated density (Mg/m^3)	1.570
Absorption coefficient (mm^{-1})	1.016
F(000)	1504
Crystal size (mm^3)	0.10 × 0.08 × 0.06
θ Range for data collection (°)	2.43–26.20
Index ranges	$-26 \le h \le 26$ $-8 \le k \le 9$ $-22 \le l \le 12$
Reflections collected	15323
Independent reflections	2723 [R(int) = 0.1086]
Completeness to θ = 25.02 (%)	99.8
Data/restraints/parameters	5489/0/406
Goodness-of-fit on F^2	1.015
Final R indices [$I > 2\sigma(I)$]	R_1 = 0.0478, wR_2 = 0.1012
R indices (all data)	R_1 = 0.0932, wR_2 = 0.1217
Largest difference peak and hole (e Å^{-3})	0.408 and –0.470

$w = 1/[\sigma^2(F_o^2) + (0.0158P)^2]$, where $P = (F_o^2 + 2F_c^2)/3$.

2.4. *Scavenger measurements of superoxide radicals*

Superoxide radicals were measured in the test system using NBT/VitB$_2$/MET [21]. HL^1 and the Ni(II) complex were dissolved in DMF (C = 4.0 μM), each solution was added to a solution containing MET (0.01 M L^{-1}), NBT (4.6 × 10^{-5} M L^{-1}), VitB$_2$ (3.3 × 10^{-6} M L^{-1}), and phosphate buffer (0.067 M L^{-1}). After incubating the mixture at 30 °C for 10 min and illuminating with a fluorescent lamp for 3 min, the absorbance (A_i) of these samples were measured at 560 nm. The results are shown in figure 8. The suppression ratio was calculated using the following equation:

$$\text{Suppression ratio}(\%) = [(A_0 - A_i)/(A_0)] \times 100\%$$

where A_i is the absorbance in the presence of HL^1 and Ni(II) complex, and A_0 is the absorbance in the absence of HL^1 and Ni(II) complex.

The antioxidant activity was described as the 50% inhibitory concentration (IC_{50}). IC_{50} values were calculated from regression lines, where x was the concentration of HL^1 and Ni (II) complex in μM and y was the percent inhibition of HL^1 and Ni(II) complex.

3. Results and discussion

3.1. *Crystal structure of $[Ni(L^2)_2]\cdot CH_3OH$*

The anticipated quinazoline-type complex $[Ni(L^1)_2]$ was not formed, but an unexpected Schiff base-type complex $[Ni(L^2)_2]$ was obtained, which was formed in the course of

complexation of HL^1 by Ni(II) acetate tetrahydrate. The ligand HL^1 changed to be a new C=N–O ligand HL^2 after forming the Ni(II) complex. In the process of reaction between Ni(II) and HL^1, unexpected cleavage of C–N bonds in HL^1 took place forming HL^2, which coordinated to Ni(II) ion forming a mononuclear Ni(II) complex with a six-membered ring Schiff base-type complex instead of an anticipated quinazoline-type Ni–N_4O_2 complex [22, 23]. The result suggests that in the metal complex the Schiff base configuration is more stable than that of quinazoline configuration (scheme 2).

X-ray structural studies reveal that the metal complex has 2 : 1 ligand to metal stoichiometry, crystallizes in the monoclinic system with $P2_1/c$ space group and consists of one Ni (II), two $(L^2)^-$, and one non-coordinated methanol. Ni(II) is bonded to oxygen and nitrogen of the two $(L^2)^-$ molecules in a *cis* arrangement in which Ni(II) is six-coordinated. The molecular structures of HL^1 and the Ni(II) complex are illustrated in figure 1, and relevant bond lengths and angles are summarized in table 2.

As shown in figure 2, the coordination environment around Ni(II) is octahedral with some distortion, by one imine nitrogen (N1), one Schiff base nitrogen (N4), and two deprotonated phenolic oxygens (O2 and O4) defining the *cis*-N_2O_2 basal plane, plus one imine nitrogen (N3) and one Schiff base nitrogen (N2) occupying apical positions from two deprotonated $(L^2)^-$ units [24, 25]. The coordination environment around Ni(II) is best regarded as a slightly distorted octahedral geometry with the distance of the apical N2 and N3 to the N_2O_2 basal plane being 1.991(4) and 2.042(4) Å. The Ni is in the N_2O_2 basal plane. The bond lengths of Ni–O are longer than Ni–N. These structural features, from steric hindrance of the L^{1-} fragments, account for the distortion of the ligand in the Ni(II) complex. The dihedral angle between two six-membered rings of methylene as vertex is 81.14(3)°. After formation of the Ni(II) complex, the dihedral angle turns to 69.30(3)°, while the dihedral angles between every two metal chelating rings adjacent to each other (the plane defined by Ni1O2C11C10C9N2, the adjacent plane defined by Ni1N1C2C3C4N2Ni1 and Ni1O4C26C25C24N2, the other adjacent plane defined by Ni1N3C17C18C19N4Ni1) for the Ni(II) complex are 51.63(3)° and 50.85(3)°, respectively.

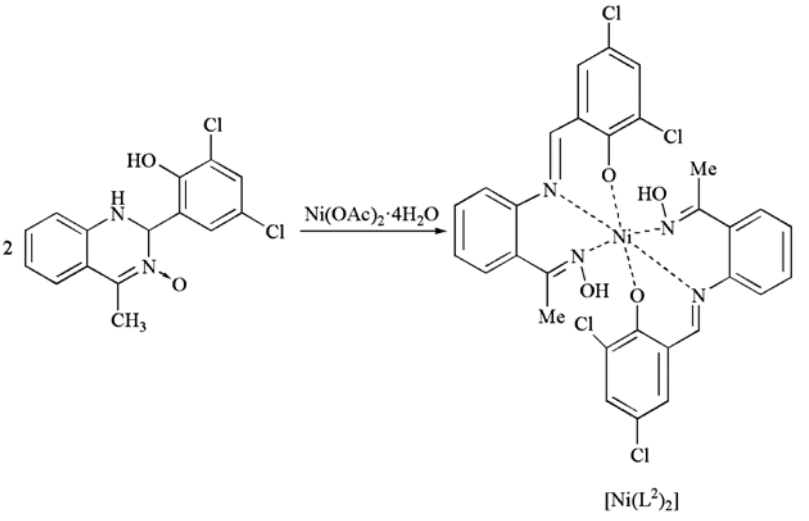

Scheme 2. Complexation of HL^1 with Ni(II) acetate.

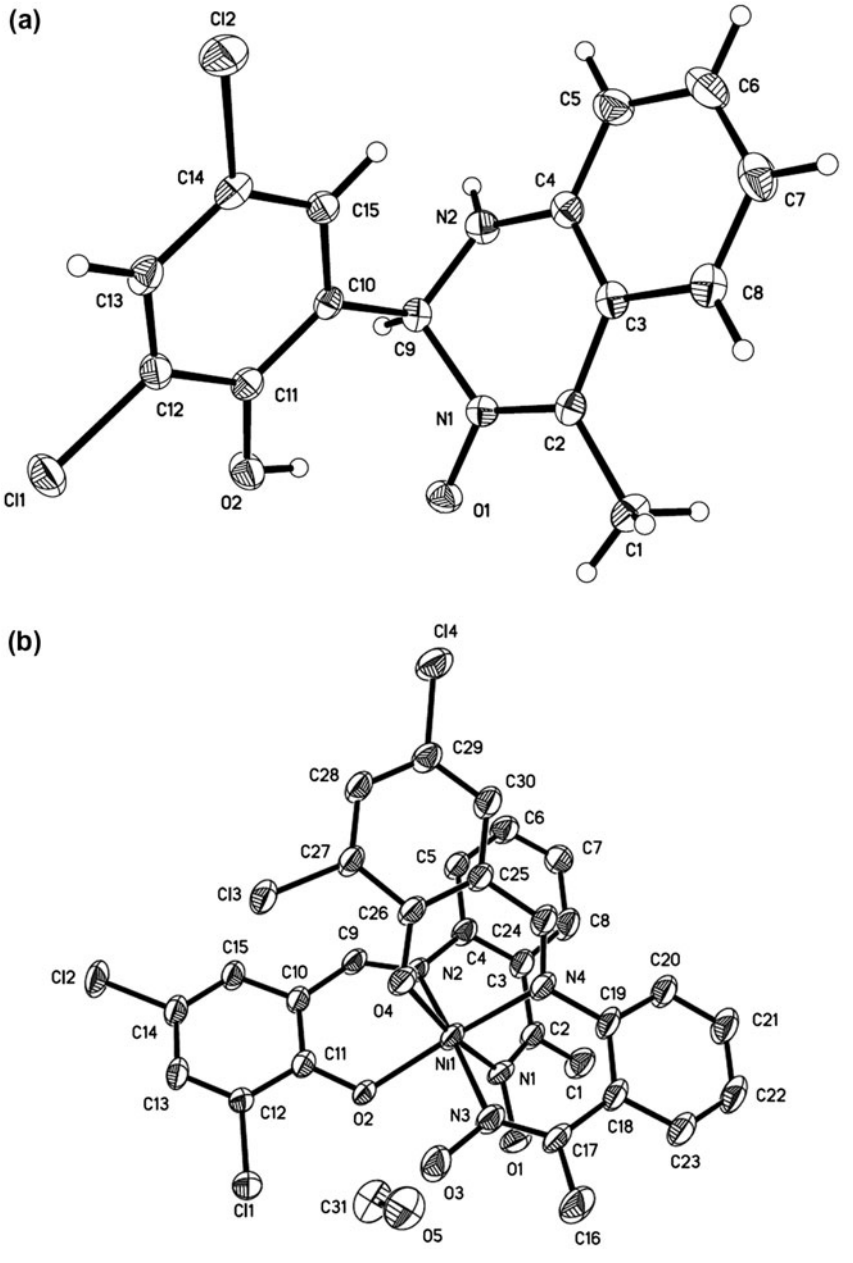

Figure 1. Crystal structures of HL^1 (a) and the Ni(II) complex (b) with atom numbering. Displacement ellipsoids for non-H atoms are drawn at the 30% probability level.

Molecules of complex are connected by intramolecular C–H···O and O–H···O hydrogen bonds (figure 3), intermolecular hydrogen bonds, and C–X···π (Ph) interactions (table 3), which play a role in stabilizing the structure of the crystal. Two pairs of intermolecular O3–H3···O2 and C1–H1A···O1 hydrogen bonds form two five-membered rings. Three

Table 2. Selected bond distances (Å) and angles (°) for the Ni(II) complex.

Bond	Dist.	Bond	Dist.	Bond	Dist.
Ni1–O2	1.999(5)	Ni1–N2	2.009(5)	Ni1–N4	2.042(6)
Ni1–O4	2.043(5)	Ni1–N3	2.047(5)	Ni1–N1	2.130(6)
Bond	Angles	Bond	Angles	Bond	Angles
O2–Ni1–N2	89.8(2)	O2–Ni1–N4	166.6(2)	N2–Ni1–N4	101.3(2)
O2–Ni1–O4	87.7(2)	N2–Ni1–O4	91.1(2)	N4–Ni1–O4	84.5(2)
O2–Ni1–N3	86.8(2)	N2–Ni1–N3	172.9(3)	N4–Ni1–N3	83.0(2)
O4–Ni1–N3	95.0(2)	O2–Ni1–N1	97.4(2)	N2–Ni1–N1	79.8(2)
N4–Ni1–N1	92.1(2)	O4–Ni1–N1	169.5(2)	N3–Ni1–N1	94.4(2)
C2–N1–Ni1	123.9(6)	O1–N1–Ni1	120.9(4)	C9–N2–Ni1	123.5(5)
C4–N2–Ni1	116.6(5)	C17–N3–Ni1	131.0(6)	O3–N3–Ni1	115.0(4)
C24–N4–Ni1	123.2(5)	C19–N4–Ni1	117.1(5)	C11–O2–Ni1	123.1(4)
C26–O4–Ni1	116.0(4)				

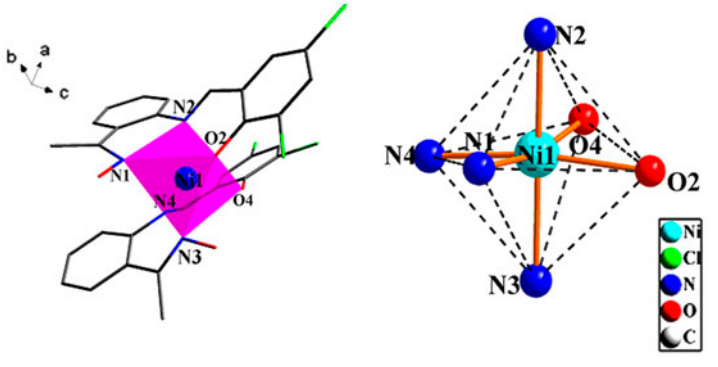

Figure 2. Coordination configuration of Ni(II) complex.

intermolecular O1–H1···O5, O5–H5···O2 and C7–H7···O4 hydrogen bonds between aromatic carbon, phenolic oxygen, and non-coordinated methanol form a seven-membered ring. A pair of C27–Cl3···Cg(6) hydrogen bonds exist between aromatic rings [26]. Intermolecular C–X···π (Ph) hydrogen bonds play an important role in stabilizing the crystal structure. With the help of hydrogen bonds, adjacent molecular units are linked by interactions to give an infinite 1-D chain supramolecular structure along the *b*-axis, as shown in figure 4.

3.2. *IR spectra*

The main FT-IR absorptions of HL^1 and the Ni(II) complex from 400 to 4000 cm^{-1} are given in table 4. The free ligand exhibits a characteristic C=N stretch at 1600 cm^{-1}, while C=N of the Ni(II) complex is observed at 1614 cm^{-1}. The C=N stretch is shifted to higher frequency by *ca.* 14 cm^{-1} upon complexation, indicating a decrease in C=N bond order due to the coordination of Ni(II) with oxime nitrogen [27]. The Ar–O stretch is a strong band at 1263–1213 cm^{-1} as reported for similar ligands [28–30], occurring at 1258 cm^{-1} for HL^1 and at 1230 cm^{-1} for the Ni(II) complex. The Ar–O stretching frequency shifts to lower frequency, indicating that Ni–O bond was formed between Ni(II) and oxygen of the phenol [31].

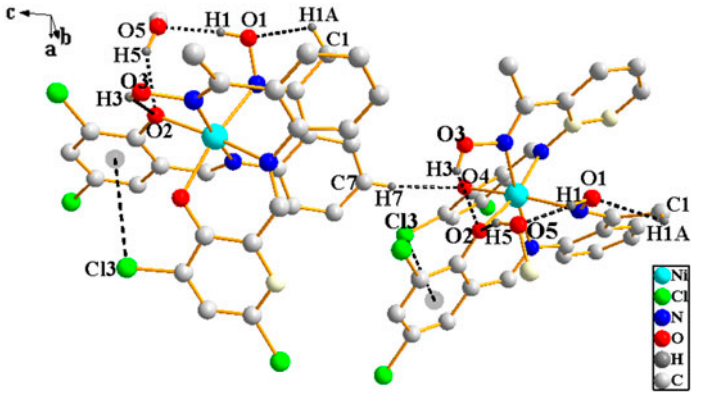

Figure 3. Hydrogen bonds of the Ni(II) complex.

Table 3. Hydrogen-bonding distances (Å) and angles (°) for the Ni(II) complex.

D–H···A	*d*(D–H)	*d*(H···A)	*d*(D···A)	<D–H···A
O3–H3···O2	0.82	2.06	2.709(7)	136
C1–H1A···O1	0.96	2.26	2.5975	100
O1–H1···O5	0.82	1.84	2.654(8)	174
O5–H5···O2	0.82	1.89	2.601(7)	145
C7–H7···O4^{i}	93	2.57	3.493(9)	170
C27–Cl3···Cg(6)^{ii}	1.73	3.76	4.616(8)	109

Symmetry code: (i) *x*, ½ − *y*, −1/2 + *z*; (ii) *x*, *y*, *z*. Cg(6) is the centroid for benzene ring C10–C15.

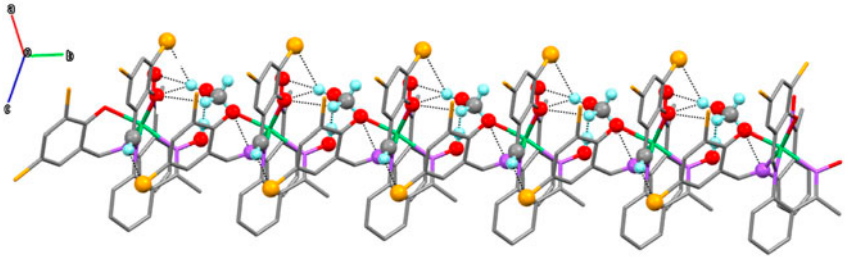

Figure 4. View of the 1-D chain motif of the Ni(II) complex along the *b*-axis.

Table 4. Selected FT-IR bands for the ligand and its Ni(II) complex (cm^{-1}).

Compound	$\nu_{(O-H)}$	$\nu_{(N-H)}$	$\nu_{(C=N)}$	$\nu_{N\rightarrow O}$	ν_{Ar-O}	$\nu_{(Ni-N)}$	$\nu_{(Ni-O)}$
HL[1]	3225	3067	1600	1278	1258	–	–
Complex	3434	–	1614	–	1230	526	423

The IR spectrum of HL[1] shows unexpected strong absorption due to ν(N→O) at 1278 cm^{-1}, which disappears in the complex, indicating the C–N bond in the Ni(II) complex has broken and oxime N participated in coordination. The N–H in HL[1] at 3067 cm^{-1} disappears in the

complex, indicating the nitrogen coordinated to Ni(II). The O–H stretch of free HL^1 appears at 3225 cm^{-1}, while the infrared spectrum of the Ni(II) complex shows the expected strong absorption due to ν(O–H) at 3434 cm^{-1}, which is evidence of O–H from oxime.

The far-infrared spectrum of the Ni(II) complex is obtained from 100–500 cm^{-1} to identify frequencies due to Ni–O and Ni–N. The FT-IR spectrum of the complex shows ν(Ni–N) and ν(Ni–O) at 526 and 423 cm^{-1}, respectively.

3.3. *UV–vis absorption spectra*

UV–vis absorption spectra of HL^1 and the Ni(II) complex were determined in 5×10^{-5} $M\,L^{-1}$ DMF solution. Absorptions of the Ni(II) complex were different from those of HL^1 as shown in figure 5. Compared with the Ni(II) complex, an important feature of the absorption spectrum of HL^1 was that three absorptions were observed at 241, 305, and 364 nm, respectively. The latter absorptions were absent in the spectrum of the Ni(II) complex. The absorption at 254 nm in the Ni(II) complex could be due to the d–d transition of Ni(II). The Ni(II) complex with $3d^8$ electronic configuration could be assigned to $^3A_{2g} \rightarrow {}^3T_{1g}$ transition of Ni(II) in an octahedral environment [32]. These observations were in line with common spectral features of d-block metal complexes [33]. The intense band near 439 nm was assigned for ligand-to-metal charge transfer transitions [32].

3.4. *Fluorescence spectra*

Fluorescent properties of HL^1 and its corresponding Ni(II) complex were investigated at room temperature (figure 6). The ligand exhibits two intense emissions at 427 and 472 nm upon excitation at 364 nm, which should be assigned to the intraligand π–π* transition [34, 35]. The Ni(II) complex shows an intense broad photoluminescence with maximum emission at *ca.* 484 nm upon excitation at 437 nm, which is red-shifted to that of HL^1. This

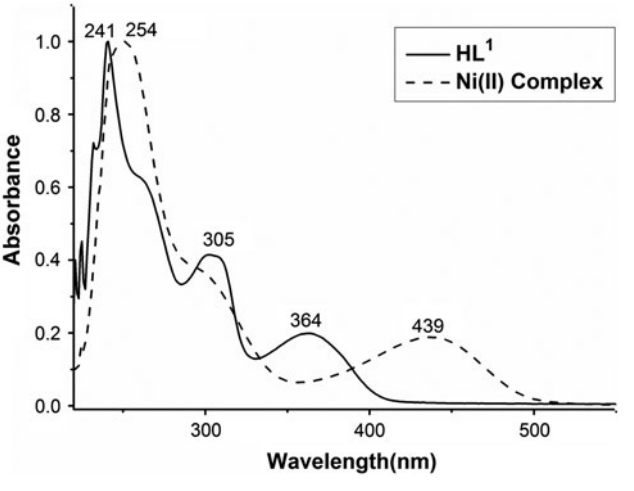

Figure 5. UV–vis absorption spectra: HL^1 (solid line) and the Ni(II) complex (dashed line) in DMF (5×10^{-5} $M\,L^{-1}$).

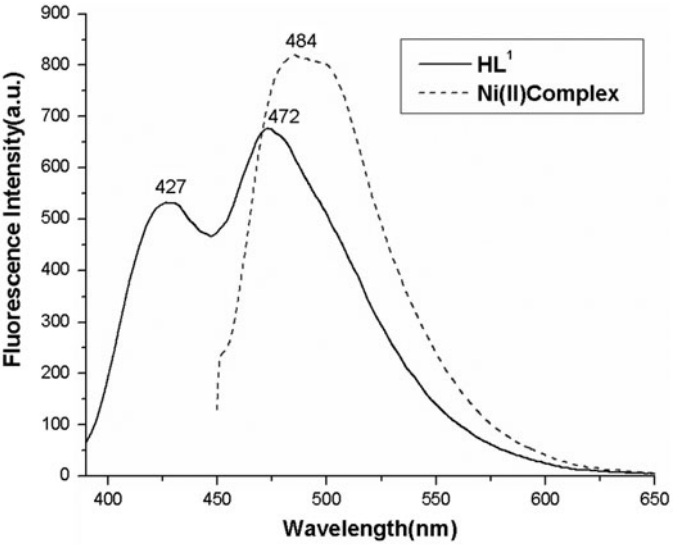

Figure 6. Emission spectra of HL^1 (solid line) and corresponding Ni(II) complex (dashed line) in dilute DMF at room temperature ($c = 5 \times 10^{-5}$ M L^{-1}).

red shift might be related to the auxochrome group (–Cl), which makes the conjugated system larger. The compounds emit strong fluorescence in the blue light area and may be potential functional fluorescent material which can emit blue light.

3.5. *Electrochemical studies*

The electrochemical property of the Ni(II) complex has been studied in DMF containing 0.05 M L^{-1} tetrabutylammonium perchlorate over the potential range from –2 to 0.7 V (*vs.* Ag/AgCl) using CV techniques, with scanning rate of 100 mV s^{-1}. As it observed in figure 7, the Ni(II) complex exhibits two reversible redox waves, which are assigned to consecutive Ni(II)/Ni(I) and Ni(III)/Ni(II) redox processes [36]. The first pair of oxidation–reduction peaks correspond to the oxidation–reduction couples Ni(III)/Ni(II), $Epa_1 = 0.197$ V, $Epc_1 = –0.896$ V, with the average formal potential [$E_{1/2} = (Epa_1 + Epc_1)/2$] is –0.347 V. The peak-to-peak separation between the anodic and cathodic processes (ΔEp_1) is 1.093 V and the proportion of the peak current (ipc_1/ipa_1) is 1.523. The second pair of oxidation–reduction peaks correspond to Ni(II)/Ni(I), $Epa_2 = –0.724$ V, $Epc_2 = –1.560$ V, with the average formal potential [$E_{1/2} = (Epa_2 + Epc_2)/2$] of 1.142 V, the peak-to-peak separation between the anodic and cathodic processes (ΔEp_2) of 0.836 V and the proportion of the peak current (ipc_2/ipa_2) of 0.771. These features are indicative of a quasi-reversible electrode process [37].

3.6. *SOD-like activity*

The SOD-like activities of HL^1 and Ni(II) complex were investigated (figure 8). The average suppression ratio against $O_2^{\cdot-}$ increases with increasing concentration in the range of the tested concentration. The observed IC_{50} values of the compounds were compared with earlier reported values for nickel(II) complexes [38, 39]. The catalytic activity of NiSOD [40],

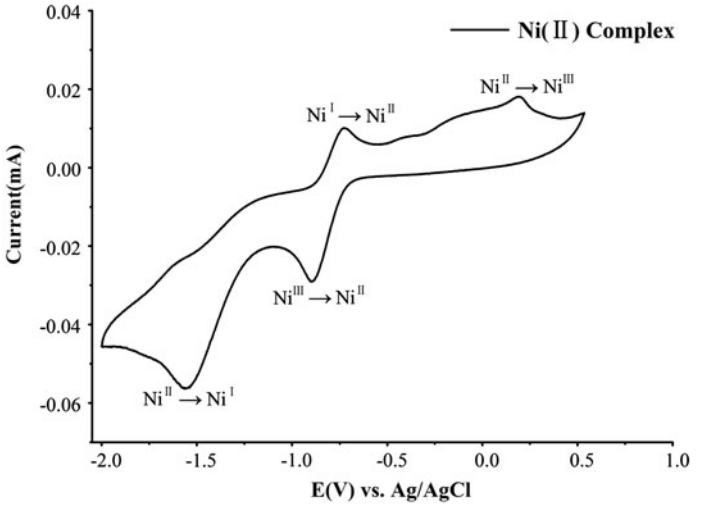

Figure 7. Cyclic voltammogram of Ni(II) complex in DMF solution. Scan rate at 100 mV s^{-1}.

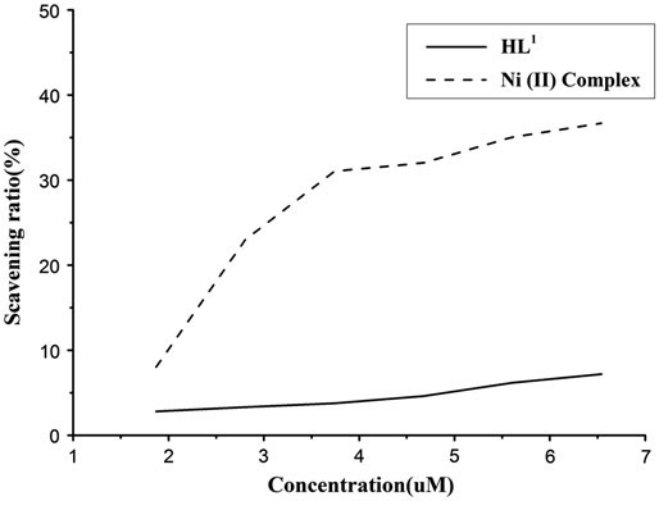

Figure 8. Scavenging effects of HL^1 (solid line) and corresponding Ni(II) complex (dashed line) on $O_2^{\cdot-}$.

however, is on the same high level as that of Cu–ZnSOD at about 109 $(M\,L^{-1})^{-1}s^{-1}$ per metal center. The IC_{50} data of the SOD activity assay along with kinetic catalytic constants of compounds [41, 42] are presented in table 5. The results indicate that the prepared compound is more efficient antioxidant than vitamin C, which is the standard superoxide dismutase [43–45]. The brown color of the octahedral Ni(II) complex exhibits more active scavenging effects against $O_2^{\cdot-}$ than HL^1 and other nickel complexes under the same conditions. The scavenging effect of the Ni(II) complex may be ascribed to the chelating function of ligand with metal ion to achieve significant selectivity of radical scavenging activity [46].

Table 5. IC_{50} values and kinetic constant of compounds.

Compound	IC_{50} (μM)	k_{McCF} $((M\,L^{-1})^{-1}s^{-1}) \times 10^4$	Refs.
Vc	852	–	[43]
HL^1	51.60	–	This work
$[Ni(L^2)_2]\cdot CH_3OH$	8.26	33.08	This work
$[Ni(L)_2]$	31	3.06	[38]
$[Ni(L)(HL)](ClO_4)(H_2O)$	34	1.76	[38]
$Ni(HL)(bipy)(H_2O)(NO_3)(ClO_4)(H_2O)$	38	2.5	[38]
$Ni(HL)(dien)(ClO_4)(H_2O)$	95	1.0	[38]
$[Ni(L^1)_2]\cdot 2H_2O$	35	2.71	[39]
$[Ni(L^2)_2](ClO_4)_2$	55	1.73	[39]
$[Ni(L^3)(bipy)](ClO_4)_2$	60	1.58	[39]

k_{McCF} were calculated by $K = k_{NBT} \times [NBT]/IC_{50}$, k_{NBT} (pH 7.8) $= 5.94 \times 10^4$ $(M\,L^{-1})^{-1}s^{-1}$ [42].

4. Conclusion

We have reported the synthesis and structural characterization of an unexpected mononuclear Ni(II) complex based on analytical and spectral data. Ni(II) caused cleavage of C–N bonds in HL^1, giving a new C=N–O ligand HL^2, which coordinates to Ni(II) forming $Ni–N_4O_2$ complex with a Schiff base-type instead of an anticipated quinazoline complex. Moreover, the quasi-reversible one-electron Ni(III)/Ni(II) and Ni(II)/Ni(I) redox waves were determined by cyclic voltammetry. In addition, the Ni(II) complex exhibits more active scavenging effects against $O_2^{\cdot-}$ than HL^1 and other nickel complexes under the same conditions. Analytic, spectroscopic, electrochemical, and crystal structure determinations show that nickel(II) has octahedral geometry.

Supplementary material

Further details of the crystal structure investigation(s) may be obtained from the Cambridge Crystallographic Data Center, Postal Address: CCDC, 12 Union Road, Cambridge CB2 1EZ, UK (Telephone: (44) 01223 762910; Facsimile: (44) 01223 336033; E-mail: deposit@ccdc.cam.ac.uk on quoting the depository number CCDC 886495).

Funding

We are thankful for the financial support by the Natural Science Foundation of Gansu Province [No: 1107RJZA165]; the Young Scholars Science Foundation of Lanzhou Jiaotong University [No: 2011038]; and the Innovation and Technology Fund of Lanzhou Jiaotong University [No: DXS-2013035].

References

[1] D.M. Boghaei, A. Bezaatpour, M. Behzad. *J. Mol. Catal. A*, **245**, 12 (2006).
[2] G. Dilber, H. Kantekin, N. Yayli, R. Abbasoğlu. *J. Coord. Chem.*, **64**, 3679 (2011).
[3] P. Zhichkin, E. Kesicki, J. Treiberg, L. Bourdon, M. Ronsheim, H.C. Ooi, S.T. White, A. Judkins, D. Fairfax. *Org. Lett.*, **9**, 1415 (2007).

[4] Merck, Co Inc., European Patent EP 0530994 A1: Quinazoline derivatives as inhibitors of HIV reverse transcriptase, Bulletin 10. 03 (1993).
[5] Z.H. Chohan, S.H. Sumrra, M.H. Youssoufi, T.B. Hadda. *Eur. J. Med. Chem.*, **45**, 2739 (2010).
[6] W.K. Dong, X.N. He, H.B. Yan, Z.W. Lv, X. Chen, C.Y. Zhao, X.L. Tang. *Polyhedron*, **28**, 1419 (2009).
[7] R. Alonso, A. Caballero, P.J. Campos, D. Sampedro, M.A. Rodríguez. *Tetrahedron*, **66**, 4469 (2010).
[8] E.M. Olasik, K.B. Świątkiewiz, E. Żurek, U. Krajewska, M. Różalski, T.J. Bartczak. *Arch. Pharm. Pharm. Med. Chem.*, **337**, 239 (2004).
[9] W.K. Dong, Y.X. Sun, Y.P. Zhang, L. Li, X.N. He, X.L. Tang. *Inorg. Chim. Acta*, **362**, 117 (2009).
[10] W.K. Dong, J.G. Duan, Y.H. Guan, J.Y. Shi, C.Y. Zhao. *Inorg. Chim. Acta*, **362**, 1129 (2009).
[11] P.G. Lacroix. *Eur. J. Inorg. Chem.*, **339**, (2001).
[12] M. Sebastian, V. Arun, P.P. Robinson, P. Leeju, G. Varsha, D. Varghese, K.K.M. Yusuff. *J. Coord. Chem.*, **64**, 525 (2011).
[13] J.M. Xiao, W. Zhang. *Inorg. Chem. Commun.*, **12**, 1175 (2009).
[14] M. Rajasekar, S. Sreedaran, R. Prabu, V. Narayanan, R. Jegadeesh, N. Raaman, A.N. Kalilur RahimanRaaman. *J. Coord. Chem.*, **63**, 136 (2010).
[15] M. Kalanithi, M. Rajarajan, P. Tharmara. *J. Coord. Chem.*, **64**, 842 (2011).
[16] L.Q. Chai, Y.L. Zhang, K. Cui, Z.R. Wang, L.W. Zhang, Y.Z. Zhang. *Z. Kristallogr. – New Cryst. Struct.*, **227**, 153 (2012).
[17] Aus dem Chemisch-Pharmazeutischen Forschungsinstitut Cluj (Klausenburg), Rumänien. Eine neue synthese fiir chinazolin-N^3-oxyde und 1.2-dihydro-chinazolin-N^3-oxyde, KöVENDI und KIRCZ, **98**, 1049 (1965).
[18] Bruker. *SAINT and SMART*, Bruker AXS Inc., Madison, WI (2001).
[19] G.M. Sheldrick. *SADABS*., University of Göttingen, Göttingen (2001).
[20] G.M. Sheldrick. *Acta Crystallogr. A*, **64**, 112 (2008).
[21] C.C. Winterbourn. *Biochem. J.*, **182**, 625 (1979).
[22] W.K. Dong, X. Chen, Y.X. Sun, X.N. He, Z.W. Lv, H.B. Yan, X.L. Tang, C.Y. Zhao. *Chin. J. Inorg. Chem.*, **24**, 1325 (2008).
[23] M.M. Carthy, P.J. Gyiry. *Polyhedron*, **19**, 541 (2000).
[24] W.K. Dong, Y.X. Sun, X.N. He, J.F. Tong, J.C. Wu. *Spectrochim. Acta, Part A*, **76**, 476 (2010).
[25] W.K. Dong, J.F. Tong, Y.X. Sun, J.C. Wu, J. Yao, S.S. Gong. *Transition Met. Chem.*, **35**, 419 (2010).
[26] D. Hauchecorne, N. Nagels, B.J. van der Vekena, W.A. Herrebout. *Phys. Chem. Chem. Phys.*, **14**, 681 (2012).
[27] W.K. Dong, S.J. Xing, Y.X. Sun, L. Zhao, L.Q. Chai, X.H. Gao. *J. Coord. Chem.*, **65**, 1212 (2012).
[28] A. Anthonysamy, S. Balasubramanian. *Inorg. Chem. Commun.*, **8**, 908 (2005).
[29] M. Asadi, K. Mohammadi, S. Esmaielzadeh, B. Etemadi, H.K. Fun. *Inorg. Chim. Acta*, **362**, 4913 (2009).
[30] L. Zhao, X.T. Dong, Y.X. Sun, Q. Chen, X.Y. Dong, L. Wang. *Chin. J. Inorg. Chem.*, **28**, 2413 (2012).
[31] T.Z. Yu, K. Zhang, Y.L. Zhao, C.H. Yang, H. Zhang, L. Qian, D.W. Fan, W.K. Dong, L.L. Chen, Y.Q. Qiu. *Inorg. Chim. Acta*, **361**, 233 (2008).
[32] C.J. Dhanaraj, J. Johnson, J. Joseph, R.S. Joseyphus. *J. Coord. Chem.*, **66**, 1416 (2013).
[33] S.M. Saadeh. *J. Coord. Chem.*, **65**, 3075 (2012).
[34] L.Q. Chai, G. Wang, Y.X. Sun, W.K. Dong, L. Zhao, X.H. Gao. *J. Coord. Chem.*, **65**, 1621 (2012).
[35] C.Y. Guo, Y.Y. Wang, K.Z. Xu, H.L. Zhu, P. Liu, Q.Z. Shi, S.M. Peng. *Polyhedron*, **27**, 3529 (2008).
[36] D.C. Olson, J. Vasilevskis. *Inorg. Chem.*, **8**, 1611 (1969).
[37] J.C. Liu, J. Cao, W.T. Deng, B.H. Chen. *J. Chem. Crystallogr.*, **41**, 806 (2011).
[38] R.N. Patel, A. Singh, V.P. Sondhiya, Y. Singh, K.K. Shukla, D.K. Patel, R. Pandey. *J. Coord. Chem.*, **65**, 795 (2012).
[39] R.N. Patel, K.K. Shukla, A. Singh, M. Choudhary, D.K. Patel, J. Niclós-Gutiérrez, D. Choquesillo-Lazarte. *J. Coord. Chem.*, **63**, 3648 (2010).
[40] H.D. Youn, E.J. Kim, J.H. Roe, Y.C. Hah, S.O. Kang. *Biochem. J.*, **318**, 889 (1996).
[41] Z.R. Liao, X.F. Zheng, B.S. Luo, L.R. Shen, D.F. Li, H.L. Liu, W. Zhao. *Polyhedron*, **20**, 2813 (2001).
[42] R.F. Pasternock, B. Halliwell. *J. Am. Chem. Soc.*, **101**, 1026 (1979).
[43] Y. Li, Z.Y. Yang, J.C. Wu. *Eur. J. Med. Chem.*, **45**, 5692 (2010).
[44] J. Cao, J.C. Liu, W.T. Deng, N.Z. Jin. *CrystEngComm*., **15**, 6359 (2013).
[45] R. Xing, H.H. Yu, S. Liu, W.W. Zhang, Q.B. Zhang, Z. Li, P.C. Li. *Bioorg. Med. Chem.*, **13**, 1387 (2005).
[46] Y.-H. Zhou, W.-Q. Wan, D.-L. Sun, J. Tao, L. Zhang, X.-W. Wei. *Z. Anorg. Allg. Chem.*, (2013). doi:10.1002/zaac.201300238.